Mon. Not. R. Astron. Soc. **000**, 000–000 (0000) Printed 2 February 2008 (MN LaTeX style file v2.2)

arXiv:astro-ph/0411778v2 1 Aug 2005

Supernovae in Helium Star–Compact Object Binaries: A Possible γ-ray Burst Mechanism

Avery E. Broderick*
Institute for Theory and Computation, Harvard-Smithsonian Center for Astrophysics, 60 Garden St., MS 51, Cambridge, MA 02138, USA

2 February 2008

ABSTRACT
Helium star–compact object binaries, and helium star–neutron star binaries in particular, are widely believed to be the progenitors of the observed double neutron star systems. In these, the second neutron star is presumed to be the compact remnant of the helium star supernova. Here, the observational implications of such a supernova are discussed, and in particular are explored as a candidate γ-ray burst mechanism. In this scenario the supernova results in a transient period of rapid accretion onto the compact object, extracting via magnetic torques its rotational energy at highly super-Eddington luminosities in the form of a narrowly beamed, strongly electromagnetically dominated jet. Compton scattering of supernova photons advected within the ejecta, and photons originating at shocks driven into the ejecta by the jet, will cool the jet and can produce the observed prompt emission characteristics, including the peak–inferred isotropic energy relation, X-ray flash characteristics, subpulse light curves, energy dependent time lags and subpulse broadening, and late time spectral softening. The duration of the burst is limited by the rate of Compton cooling of the jet, eventually creating an optically thick, moderately relativistically expanding fireball which can produce the afterglow emission. If the black hole or neutron star stays bound to a compact remnant, late term light curve variability may be observed as in SN 2003dh.

Key words: gamma-rays: bursts – binaries: close – pulsars: general – supernovae: general

1 INTRODUCTION

Despite being discovered more than 30 years ago (Klebesadel et al. 1973), and the fact that bursts have been detected daily since the advent of the Compton Gamma-Ray Observatory in 1991, there still does not exist a satisfactory theoretical model which encompasses the entire γ-ray burst event. Nonetheless, in spite of their strong heterogeneity, the abundance of observations has led to a well described burst phenomenology, and is briefly summarised below.

Burst durations are bimodal, with long bursts lasting $\sim 100\,$s while short bursts last $\sim 1\,$s (Kouveliotou et al. 1993). Long bursts typically have inferred isotropic luminosities on the order of $\sim 10^{51-52}$ erg/s (see, e.g., Piran 2004, and references therein), although achromatic breaks in the afterglow light curves suggest strong collimation (with opening angles $\sim 5-10^\circ$, Frail et al. 2001) which, in turn, implies actual luminosities on the order of $\sim 10^{48-49}$ erg/s. The majority of the prompt emission is in the form of apparently nonthermal γ-rays, well fit by a broken power law, typically peaking near 100–1000 keV, and softening throughout the burst. The prompt emission is composed of a large number of subpulses with typical widths on the order of a second in which lower energy emission lag behind, and are wider than, the higher energy emission.

Long bursts are followed by optical and radio afterglows thought to be generated by a hot fireball interacting with the interstellar medium (see, e.g., Mészáros 2002; Li & Chevalier 2003). These can last many weeks and have in at least two cases (GRB 980425 and GRB 030329) included type Ib,c supernova (SN 1998bw and SN 2003dh, respectively) light curves 7–10 days after the prompt emission. The total bolometric energy in these bursts has been estimated from late time radio observations to be $\sim 10^{51}$ erg and roughly constant among bursts (Berger et al. 2004). To date, there have been no instances of afterglow or supernova being associated with short bursts.

Due to similarities in their temporal structure, duration, and spectra, X-ray flashes appear to be low luminosity cousins of γ-ray bursts. Recently it has been shown that their

---

* E-mail: abroderick@cfa.harvard.edu

© 0000 RAS

bolometric luminosity is indeed comparable to normal bursts (Soderberg et al. 2004). Despite this, their inferred isotropic energy is substantially less ($\sim 10^{49}$ erg) placing X-ray flashes upon the peak–inferred isotropic energy relation discovered by Amati et al. (2002), and supporting a unified interpretation of X-ray flashes and γ-ray bursts (Sakamoto et al. 2004).

A number of mechanisms have been suggested for γ-ray bursts. Frequently, these address either the central engine and emission separately. Central engine models include black hole and/or neutron star collisions (Eichler et al. 1989; Paczynski 1991; Narayan et al. 1992), magnetar birth (Usov 1992; Thompson 1994; Thompson et al. 2004), black hole birth (Vietri & Stella 1998), and collapsar (see, e.g., MacFadyen et al. 2001) models. In most of these it is not clear how the spectral and temporal structure of the burst is produced. In contrast, there are also a number of models which focus upon the emission. These include the cannonball (Dado et al. 2002, and references therein), shot gun (Heinz & Begelman 1999), Comptonised jet (Thompson 1994; Ghisellini et al. 2000), and internal shock (Piran 2004) models. Despite their ability to reproduce many of the observed spectral and temporal features of the bursts, few of these address directly the power source of the burst. As a result, currently there are few models which can explain both the properties of the observed emission and the prodigious energy of observed bursts in a satisfactory manner.

Here a model involving supernovae in helium star–black hole and helium star–neutron star binaries is presented. In this scenario the supernova results in a transient period of rapid accretion onto the compact object, extracting via magnetic torques its rotational energy at highly super-Eddington luminosities in the form of a narrowly beamed, strongly electromagnetically dominated jet. The prompt emission is produced by Compton scattering supernova photons advected within the ejecta and photons created at shocks driven into the ejecta by the jet. The duration of the burst is limited by the rate of Compton cooling of the jet, eventually creating an optically thick, moderately relativistically expanding fireball which can produce the afterglow emission. In comparison with the previous models this has two advantages: firstly it provides a unified model for the central engine and the prompt emission, and secondly, since helium star–neutron star binaries are widely believed to be the progenitors of the observed double pulsars, it is assured that supernova in these systems will occur in sufficient quantity (see section 3.5). For convenience, typical values for the pertinent quantities which describe the model are collected in Table 1 and a schematic of the process is shown in Figure 1.

The formation and energetics of the jet are discussed in Section 2. Sections 3 and 4 describe the mechanisms by which the kinetic energy of the jet is converted in the the observed prompt emission and subsequent afterglow, including the limits this places upon the jet dynamics. Expected observational implications of this model are discussed in Section 5. Finally, concluding remarks are contained in Section 6.

Helium Star Mass	$M_{\rm He}$	$2\,M_\odot$
Helium Star Radius	$R_{\rm He}$	2×10^{11} cm
Orbital Separation	a	4×10^{11} cm
Supernova Ejecta Density	$\rho_{\rm sn}$	10^{-2} g/cm^3
Supernova Ejecta Velocity	$v_{\rm sn}$	10^3 km/s
Neutron Star Mass	$M_{\rm NS}$	$1.4\,M_\odot$
Neutron Star Radius	$R_{\rm NS}$	10^6 cm
Black Hole Mass	$M_{\rm BH}$	$10\,M_\odot$
Jet Lorentz Factor	Γ	20
Jet Plasma σ	σ	10^4

Table 1. A number of model parameters are listed together with some of the jet characteristics obtained in the following sections.

2 JET FORMATION

A high power jet (or highly collimated relativistic outflow) is a central feature of most γ-ray burst models. Observational constraints require that the luminosity of a jet with opening angle $\sim\Gamma^{-1}$ (where Γ is the bulk Lorentz factor) be on the order of

$$L_{\rm jet} \simeq \frac{1}{4\Gamma^2}L_{\rm iso} \simeq 6\times10^{47}\left(\frac{\Gamma}{20}\right)^{-2}\left(\frac{L_{\rm iso}}{10^{51}\,{\rm erg/s}}\right)\,{\rm erg/s}\,, \tag{1}$$

where $L_{\rm iso}$ is the isotropic equivalent luminosity of the burst. For a burst of duration T, this corresponds to a total energy budget of

$$E_{\rm tot} \simeq 6\times10^{49}\left(\frac{\Gamma}{20}\right)^{-2}\left(\frac{L_{\rm iso}}{10^{51}\,{\rm erg/s}}\right)\left(\frac{T}{100\,{\rm s}}\right)\,{\rm erg}\,. \tag{2}$$

The observational features of the model presented here depend only upon the existence of a suitably luminous and electromagnetically pure jet (see, e.g., section 3.2) in the vicinity of the supernova, and are otherwise independent of the mechanism by which such a jet is produced. Nonetheless, for concretness, here the jet is presumed to be the result of accretion driven electromagnetic torques upon a central compact object. Therefore, possible mechanisms for the production of such a jet are discussed below in the cases where the compact object is a black hole or a neutron star. However, this is in no means meant to be an exhaustive discussion of the problem of jet formation, which is beyond the scope of this paper.

2.1 Black Hole Binaries

A considerable literature exists regarding the production of jets via the electromagnetic extraction of angular momentum from accreting black holes (see, e.g., Blandford & Znajek 1977; McKinney & Gammie 2004; Komissarov 2004; Levinson 2005, and references therein). The maximum energy that may be extracted by this method is determined by the irreducible mass, $M_{\rm ir}$:

$$\begin{aligned} E_{\rm tot} &= M_{\rm BH}c^2\left(1-\frac{M_{\rm ir}}{M_{\rm BH}}\right) \\ &\simeq \frac{1}{8}j^2M_{\rm BH}c^2 \\ &\simeq 10^{55}j^2\,{\rm erg}\,. \end{aligned} \tag{3}$$

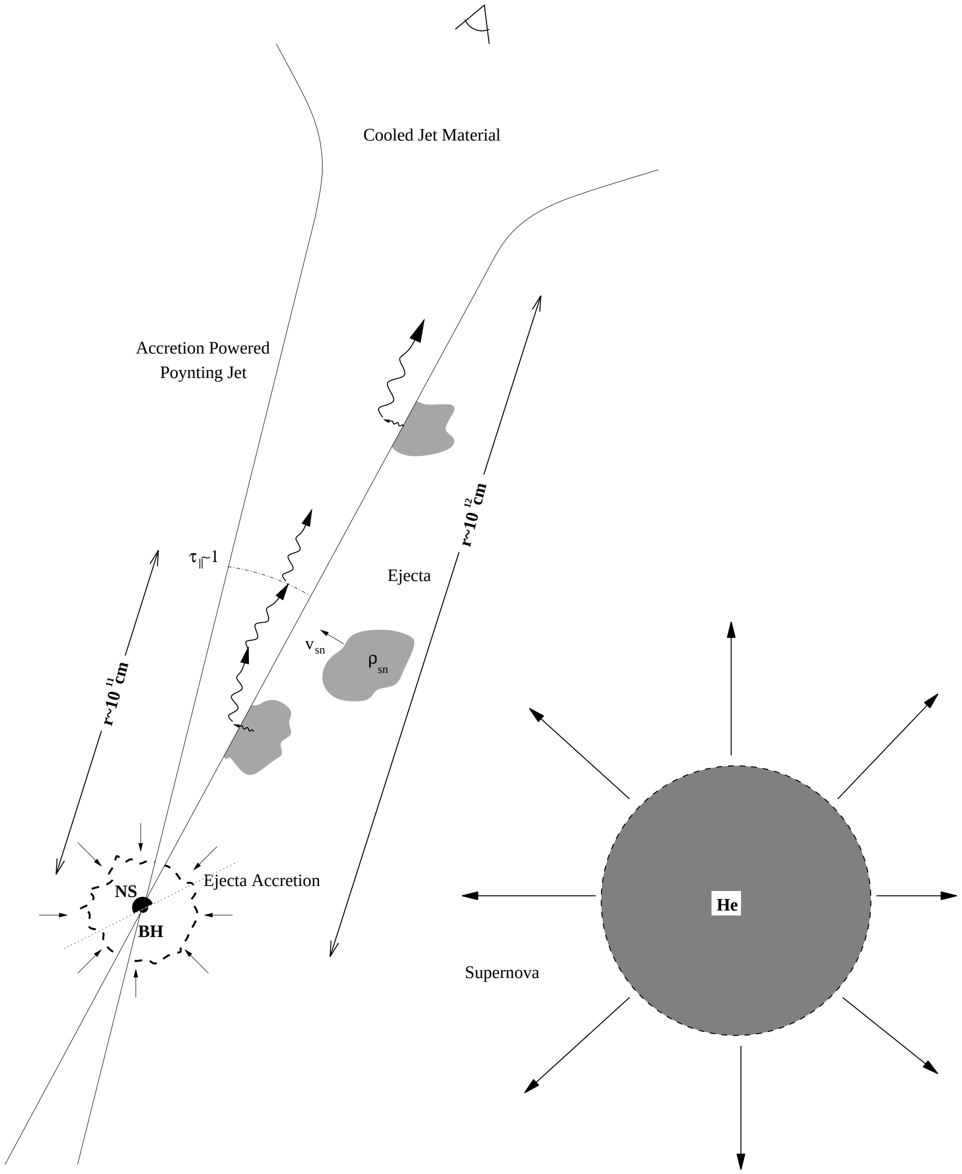

Figure 1. A cartoon of the mechanism is shown (not to scale) with the principle features, supernova ejecta, accretion driven jets, up-scattered entrained and shock produced photons from the ejecta, and the regions where the jet is axially optically thin ($r \sim 10^{11}$ cm) and becoming nonrelativistic.

where j is the dimensionless angular momentum of the black hole, and the expansion is appropriate for $j \ll 1$ (see, e.g., Misner et al. 1973). Comparing this to the energy required to power a burst (cf.equation 2) requires $j \gtrsim 0.01$, and thus puts a rather weak limit upon the spin of the black hole.

In the model presented here, the torque upon the black hole is due to a substantially super-Eddington accretion flow resulting from the accretion of the supernova ejecta. An estimate for the mass accretion rate in this scenario is simply given by the Bondi-Hoyle rate,

$$\begin{aligned}\dot{M} &\simeq \pi r_{\mathcal{BH}}^2 \rho_{\rm sn} v_{\rm sn} \simeq 4\pi\rho_{\rm sn}\left(\frac{GM_{\rm BH}}{c^2}\right)^2\left(\frac{v_{\rm sn}}{c}\right)^{-3} c \\ &\simeq 2\times 10^{29}\,{\rm g/s}\,, \qquad (4)\end{aligned}$$

where the Bondi-Hoyle radius is given by

$$r_{\mathcal{BH}} = \frac{2GM_{\rm BH}}{v_{\rm sn}^2 + c_s^2}\,, \qquad (5)$$

in which the sound speed (c_s) may typically be ignored compared to the ejecta bulk velocity. The resulting density in the vicinity of the horizon is then

$$\rho = \frac{\dot{M}}{4\pi r_h^2 c} \simeq \left(\frac{v_{\rm sn}}{c}\right)^{-3} \rho_{\rm sn}\,, \qquad (6)$$

where r_h is the horizon radius. This implies a magnetic field strength on the order of

$$\begin{aligned}B_{\rm BH} &\simeq \sqrt{\rho_{\rm sn} c^2}\left(\frac{v_{\rm sn}}{c}\right)^{-3/2} \\ &\simeq 2\times 10^{13}\,{\rm G}\,, \qquad (7)\end{aligned}$$

presumably created via the magneto-rotational instability (MRI) (Hawley & Balbus 1995). The rotational energy may then be electromagnetically tapped by, e.g., the Blandford-Znajek process (Blandford & Znajek 1977). Recent numerical simulations of accreting black holes have produced Poynting flux dominated jets with typical luminosities of

$$L_{\rm BH} \simeq \Omega_{\rm BH}^4 B_{\rm BH}^2 \frac{1}{c^3}\left(\frac{GM_{\rm BH}}{c^2}\right)^6 \simeq 2\times10^{48} j^4\,{\rm erg/s}\,, \tag{8}$$

where $\Omega_{\rm BH} = jc/2r_h$ is a measure of the angular velocity of the black hole (McKinney 2005). Therefore, rapidly rotating black holes ($j \gtrsim 0.8$ for the black hole parameters given here, cf. Gammie et al. 2004) are easily capable of producing a Poynting dominated jet of sufficient luminosity.

This scenario is similar to the central engine models for the collapsar scheme (see, e.g., Popham et al. 1998), the primary difference being the accretion rate. In both cases, the accretion flow is neutrino cooled, and thus able to reach substantially super-Eddington (cf. with 10^{18} g/s) accretion rates. However, whereas the typical collapsar accretion rates are on the order of $1 M_\odot\,{\rm s}^{-1}$, here they are a considerably lower $10^{-4} M_\odot\,{\rm s}^{-1}$.

2.2 Neutron Star Binaries

A second, and perhaps more speculative, mechanism by which the jet might be formed involves a rapidly rotating neutron star. As with the black hole, in this scenario the energy is provided by the spin of the star. The total rotational energy available is

$$E_{\rm tot} = \frac{1}{2} I_{\rm NS}\Omega_{\rm NS}^2 \simeq \frac{1}{5} M_{\rm NS} R_{\rm NS}^2 \Omega_{\rm NS}^2 = \frac{GM_{\rm NS}^2}{5R_{\rm NS}}\omega^2 \simeq 10^{53}\omega^2\,{\rm erg}\,, \tag{9}$$

where ω is the angular velocity in units of the breakup velocity. In order to be sufficient to power a burst this already requires that $\omega \gtrsim 0.03$ and hence the neutron star must be rapidly rotating ($P \lesssim 15\,{\rm ms}$) consistent with observations of millisecond pulsars.

As with the black hole, the accretion of the supernova ejecta may mediate the extraction of the rotational energy. In the neutron star case, the Bondi-Hoyle accretion rate is given approximately by

$$\dot{M} \simeq 5\times10^{27}\,{\rm g/s}\,, \tag{10}$$

at which, as in the black hole case, neutrino cooling dominates (Chevalier 1989; Fryer et al. 1996). Near the neutron star, this results in a density on the order of

$$\rho \simeq \frac{\dot{M}}{4\pi R_{\rm NS}^2 v_r} \simeq 10^4 \beta_r^{-1}\,{\rm g\,cm^{-3}}\,, \tag{11}$$

where $v_r \equiv \beta_r c$ is the infall velocity near the neutron star surface. This implies an accretion magnetic field strength on the order of

$$B_{\rm NS} \simeq 4\times10^{12}\beta_r^{-1/2}\,{\rm G}\,. \tag{12}$$

Note that this is a lower limit as the radial infall velocity may be substantially less than the speed of light. This field will reconnect with the native stellar field on time scales comparable to the infall time scale (Ghosh & Lamb 1979). Therefore, it may not be necessary for the native field of the neutron star to initially be dynamically significant for it to subsequently strongly couple the star to the disk.

The resulting spin-down torque has been studied primarily in the context of propellor accretion flows (see, e.g., Ghosh & Lamb 1979; Ekşi et al. 2005; Romanova et al. 2004). Unfortunately, the magnitude of the spin down-torque is not a settled issue. Nonetheless, recent numerical and analytical efforts have implied that

$$\mathcal{M} \simeq B_{\rm d}^2 R_{\rm d}^2 v_{\rm esc}\eta\left(1-\eta\right)\,, \tag{13}$$

where $R_{\rm d}$ is the radius at which the magnetic field is dominated by the inertia of the disk, $B_{\rm d}$ is the magnetic field at this radius, $v_{\rm esc}$ is the escape velocity from this radius, and η, the so-called fastness parameter, is the rotation frequency of the neutron star in units of the Keplerian velocity at the dissipation radius (Romanova et al. 2004; Ekşi et al. 2005). Clearly the minimum dissipation radius is the radius of the neutron star, and thus the maximum *possible* luminosity is

$$L_{\rm NSmax} \simeq B_{\rm NS}^2 R_{\rm NS}^2 c\,\omega\left(1-\omega\right)\,, \tag{14}$$

which is sufficient to drive a burst provided that $B \gtrsim 10^{13}$ G and ω is near unity ($P \sim 1\,{\rm ms}$). The former is satisfied if $\beta_r \simeq 0.1$. The latter must be satisfied for a propellor to operate if the dissipation radius is near the surface, placing a more stringent constraint upon the spin of the star. It should be noted that such a high spin may be expected in neutron star–helium star binaries if the helium star's hydrogen envelope was expelled due to accretion by the neutron star or common envelope evolution, as is commonly thought to be the case in such systems (Bethe & Brown 1998).

In the standard propeller theory the dissipation radius is assumed to be approximately the Alfvén radius, where the pressure from the neutron star's native field balances the accretion ram pressure. However, in the hyperaccreting millisecond pulsar case (considered here) the dominant magnetic field is the accretion flow field. Therefore, this case may be more analogous to accreting black holes (in which the dissipation radius is roughly that of the horizon) than to accreting pulsars.

The manner in which the dissipated energy is transported out of the system is not clear a priori. Numerical simulations of propellors have found the development of a magnetic chimney, suggestive of the development of a jet, suggesting that some fraction of the energy leaves in a Poynting flux (Romanova et al. 2004). This interpretation is supported by the obvious parallels with the accreting black hole case, in which a significant fraction of the spin-down energy is channeled into a Poynting jet. However, a definitive answer will depend upon the details of the accretion flow and the magnetic coupling to the star, and will likely have to await detailed numerical simulations.

2.3 Jet Emergence

In order to have observational consequences it is necessary for the jet to emerge from the growing supernova. This is analogous to the problem of jet emergence in the collapsar model (see, e.g., MacFadyen et al. 2001) with a reduction of the external medium density by eight orders of magnitude.

The ram pressure of the jet,

$$P_{\rm jet} \simeq \frac{\Gamma^2 L_{\rm jet}}{3\pi r^2 c} \simeq \frac{L_{\rm iso}}{12\pi r^2 c} \qquad (15)$$
$$\simeq 1\times10^{15}\left(\frac{L_{\rm iso}}{10^{51}\,{\rm erg/s}}\right)\left(\frac{r}{10^{12}\,{\rm cm}}\right)^{-2}\,{\rm erg/cm^3}\,,$$

can be compared to the typical pressures in the supernova ejecta,

$$P_{\rm sn} \simeq \frac{1}{6}\rho_{\rm sn} v_{\rm sn}^2 \simeq 2\times10^{13}\,{\rm erg/cm^3}\,, \qquad (16)$$

(the thermal photon pressure will be comparable at the orbital separations considered here) and hence the jet will easily escape the ejecta.

3 PROMPT EMISSION

The presence of a jet alone is insufficient to produce a γ-ray burst. Also required is a mechanism by which the considerable kinetic energy flux of the jet can be converted into the observed prompt emission. Many such mechanisms have been discussed in the literature. However, for highly beamed emission, a minimum requirement is that the jet be optically thin along the jet axis. This may be accomplished in a number of ways, including clumpy jets. However, in the context of the model considered here, in which a large number of seed photons are available entrained in the supernova ejecta, this immediately suggests inverse-Compton scattering as the prompt emission mechanism. This has the considerable advantage over internal shock scenarios of being capable of converting the kinetic energy of the jet into the prompt emission at efficiencies approaching unity (see, e.g., Lazzati et al. 1999).

3.1 Photon Collimation

Due to the high bulk Lorentz factor, the scattered seed photons will naturally be collimated to within Γ^{-1} of the jet axis (see, e.g., Begelman & Sikora 1987). However, in addition, there are optical depth effects which will also serve to beam the scattered photons.

In the rest frame of the jet electrons, the Thomson depth is given by

$$\tau = \int \sigma_T n_e c {\rm d}t'\,. \qquad (17)$$

When transformed into the lab frame this gives

$$\tau = \int \sigma_T n_e c \Gamma\left(1-\beta\cos\theta\right){\rm d}t \qquad (18)$$
$$= \int \sigma_T n_e \Gamma\left(1-\beta\cos\theta\right){\rm d}r\,,$$

where in both cases n_e is the proper electron number density. For the two limiting cases of across the jet ($\theta \gg \Gamma^{-1}$) and along the jet ($\theta \lesssim \Gamma^{-1}$), the optical depth is

$$\tau_\parallel = \frac{1}{2\Gamma}\sigma_T n_e r \qquad \theta = 0$$
$$\tau_\perp = 2\sigma_T n_e r \qquad \theta = \frac{\pi}{2}\,, \qquad (19)$$

where $n_e \propto r^{-2}$ (changing the power law index changes $\tau_\parallel$ by factors of order unity) was assumed and a jet width of $2r/\Gamma$ was used. Therefore, despite the considerable difference in scale length, the optical depth along the jet is a factor of Γ less than that across the jet. As a result, it is possible to have a jet which is optically thin to photons within $\sim\Gamma^{-1}$ of the jet axis while being optically thick to all others. This provides an additional collimating mechanism and explains why it is possible to Compton scatter a large number of the seed photons incident on the jet while allowing the scattered burst photons to escape.

3.2 Implications for Jet Type

The requirement that at interesting radii $\tau_\parallel < 1$ limits the baryon loading of the jet. The power associated with ions in the jet is

$$L_{\rm ions} \simeq \frac{\pi r^2}{\Gamma} n_e m_p c^3 \simeq \frac{2\pi r}{\sigma_T} m_p c^3 \tau_\parallel \qquad (20)$$
$$\simeq 10^{-4}\left(\frac{\Gamma}{20}\right)^2\left(\frac{r}{10^{11}\,{\rm cm}}\right)\tau_\parallel L_{\rm jet}\,.$$

Hence, the condition that the jet be optically thin along it's axis at $r \sim 10^{11}$ cm requires that in the jet,

$$\sigma \equiv \frac{L_{\rm jet}}{L_{\rm ions}} - 1 \gtrsim 10^4\,, \qquad (21)$$

where σ is the ratio the Poynting flux to the kinetic energy flux of the baryons. Therefore, the jet must be extremely electromagnetically dominated. It should be noted however that observational precedent for such an electromagnetically dominated outflow exists in the context of the Crab pulsar in which $\sigma \sim 10^6$ at these radii (see, e.g., Vlahakis 2004; Komissarov & Lyubarsky 2004).

The magnetic fields within the jet required to generate a Poynting flux with the γ-ray burst luminosities will typically be of order

$$B \simeq \sqrt{2\frac{L_{\rm iso}}{r^2 c}}$$
$$\simeq 3\times10^9\left(\frac{L_{\rm iso}}{10^{51}\,{\rm erg/s}}\right)^{1/2}\left(\frac{r}{10^{11}\,{\rm cm}}\right)^{-1}\,{\rm G}\,, \qquad (22)$$

for $r \gg R_{\rm NS}$[1]. The resulting synchrotron cooling time for an electron with Lorentz factor γ in the frame of the jet is then

$$t_{\rm syn} \simeq \frac{\gamma m_e c^2}{P_{\rm syn}} \simeq 6\pi\frac{m_e c^2}{\sigma_T c B^2}\gamma^{-1} \qquad (23)$$
$$\simeq 10^{-10}\left(\frac{L_{\rm iso}}{10^{51}\,{\rm erg/s}}\right)^{-1}\left(\frac{r}{10^{11}\,{\rm cm}}\right)^2\gamma^{-1}\,{\rm s}\,,$$

hence these electrons may always be treated as cold in this frame.

---

[1] The conical structure of the jet will not necessarily extrapolate down to the acceleration region which is expected to occur on a scale of many gravitational radii. If it were this would suggest magnetic field strengths on the order of 10^{15} G, as is suggested in magnetar models of γ-ray bursts as opposed to the far more conservative few × 10^{13} G discussed here.

3.3 Compton Seed Photons

From momentum conservation, the energy of a photon after a single Compton scatter is given by

$$\epsilon_f = \frac{1-\beta\cos\theta_i}{1-\beta\cos\theta_f+\epsilon_i\left(1-\cos\Theta\right)/\Gamma m_e c^2}\epsilon_i\,, \tag{24}$$

where $\theta_{i,f}$ are the initial and final photon propagation angle with respect to the jet axis, and Θ is the angle between the initial and final photon propagation direction. For photons scattered to within Γ^{-1} (as expected from relativistic beaming and optical depth collimation), the resulting energy is given approximately by

$$\epsilon_f = \min\left(2\Gamma^2\epsilon_i, \Gamma m_e c^2\right)\,. \tag{25}$$

Therefore, in order to generate a burst with an isotropic luminosity of $L_{\rm iso}$, a luminosity of $L_{\rm iso}/8\Gamma^4 \simeq 10^{45}(\Gamma/20)^{-4}$ erg/s of seed photons are required to impinge upon the jet.

There are two sources of seed photons, the thermal photons from the supernova itself and those produced by strong shocks driven into the ejecta by the jet. In the first case, due to the ejecta's high Thomson depth, these will be entrained in, and in thermal equilibrium with, the ejecta. Thus, assuming the ejecta cools adiabatically as it expands, the photon temperature will be

$$T_\gamma \simeq \frac{m_p v_{\rm sn}^2}{3k}\left(\frac{r}{R_{\rm He}}\right)^{-2} \simeq 4\left(\frac{r}{R_{\rm He}}\right)^{-2}\,{\rm keV}\,, \tag{26}$$

and hence the typical photon energy is on the order of 1 keV for an orbital separation of $\gtrsim 2R_{\rm He}$ which would be expected if the Helium star is filling its Roche lobe. The associated energy density of photons is

$$u_T = aT_\gamma^4 \sim 2\times10^{16}\left(\frac{r}{R_{\rm He}}\right)^{-8} \sim 10^{14}\,{\rm erg/cm^3}\,, \tag{27}$$

(where here a is the Stefan-Boltzmann constant and not to be confused with the orbital separation) and thus the luminosity of thermal seed photons available to the jet is approximately

$$L_T \sim u_T v_{\rm sn}\frac{2r^2}{\Gamma} \sim 10^{45}\left(\frac{r}{10^{12}\,{\rm cm}}\right)^2\left(\frac{\Gamma}{20}\right)^{-1}\,{\rm erg/s}\,, \tag{28}$$

where clearly this depends upon the alignment of the jet relative to the orbital plane through the dependence of u_T upon the jet position. In the second case, the kinetic energy of the ejecta is thermalised at the jet boundary providing a seed photon luminosity of roughly

$$\begin{aligned} L_S &\sim \frac{1}{2}\rho_{\rm sn}v_{\rm sn}^3\frac{2r^2}{\Gamma} \\ &\sim 10^{45}\left(\frac{r}{10^{12}\,{\rm cm}}\right)^2\left(\frac{\Gamma}{20}\right)^{-1}\,{\rm erg/s}\,, \end{aligned} \tag{29}$$

which is comparable to L_T. Depending upon the shock structure and location these may also be thermalised. Due to its weaker dependence upon r ($\rho_{\rm sn}\propto r^{-3}$) this contribution will dominate at large radii. The total luminosity of seed photons entering the jet is then simply

$$L_{\rm seed} = L_T + L_S\,, \tag{30}$$

which is sufficient.

3.4 Implications for Jet Lorentz Factor

Recent simulations suggest that in vacuum it would be expected that the jet would accelerate due to magnetic stresses until it was no longer electromagnetically dominated, i.e., Γ would approach $\sigma \sim 10^4$ (Spitkovsky & Arons 2004)[2]. If the seed photons are indeed from a thermal distribution with $T_\gamma \sim 1$ keV as argued in the previous sections, the up-scattered emission would peak at a few GeV, far higher than is observed. However, in the situation under consideration here, the Compton scattering will induce a drag on the jet, substantially reducing its velocity. This will manifest itself differently depending upon whether or not the jet is optically thin along its axis.

When it is optically thin, the rate at which energy is lost by the jet to the up-scattered photons at a given radius is simply given by the rate at which seed photons enter the jet and their subsequent up-scattered energy, i.e.,

$$\frac{{\rm d}L}{{\rm d}r} = -2\Gamma^2\frac{{\rm d}L_{\rm seed}}{{\rm d}r}\,, \tag{31}$$

where $L_{\rm seed}$ as a function of radius is defined by

$$L_{\rm seed}(r) = \int_{r_0}^{r}\left(u_T+u_S\right)v_{\rm sn}\frac{2r}{\Gamma}{\rm d}r\,, \tag{32}$$

and u_S is the energy density of seed photons produced in the shocks (of order $\rho_{\rm sn}v_{\rm sn}^2/2$). Since ${\rm d}L/{\rm d}r$ is negative definite it will generally produce a deceleration in the jet.

In contrast, when $\tau_\parallel > 1$ the up-scattered photons cannot escape. They will consequently rescatter, introducing a second term to the energy loss:

$$\frac{{\rm d}L}{{\rm d}r} = -2\Gamma^2\frac{{\rm d}L_{\rm seed}}{{\rm d}r} - 2L_{\rm seed}\frac{{\rm d}\Gamma^2}{{\rm d}r} = -\frac{{\rm d}}{{\rm d}r}2\Gamma^2L_{\rm seed}\,. \tag{33}$$

Unlike the optically thin case, for strongly decelerating jets this can produce a positive accelerating force. This provides an effective mass loading of the jet, and since σ is so high, will determine the maximum Γ reached, i.e.,

$$\begin{aligned} \Gamma &\simeq \frac{L_{\rm jet}}{2\Gamma^2 L_{\rm seed}|_{\tau_\parallel=1}} \simeq \frac{L_{\rm iso}}{8\Gamma^3\left(u_T+u_S\right)v_{\rm sn}r^2} \\ &\longrightarrow \Gamma \simeq 30\left(\frac{L_{\rm iso}}{10^{51}\,{\rm erg/s}}\right)^{1/4}\left(\frac{r}{10^{11}\,{\rm cm}}\right)^{-1/2}\,. \end{aligned} \tag{34}$$

Hence if the jet becomes optically thin near $r = 2\times10^{11}$ cm, $\Gamma \simeq 20$ as assumed thus far. After $\tau_\parallel$ drops below unity the jet will continue to decelerate until it exits the ejecta or stalls.

The Lorentz factors considered here are substantially lower than those implied by the typical resolution to the "compactness problem" (which are $\gtrsim$ few $\times\ 10^2$, see, e.g., Lithwick & Sari 2001). The runaway pair production associated with the "compactness problem" is not present here as a result of the low energy of the seed photons themselves. In the jet frame, the seed photons have energy $\sim \Gamma\epsilon_{\rm sn}$, where $\epsilon_{\rm sn}$ is the typical seed photon energy in the lab frame. Since in the jet frame the electrons are cold, and thus all of the photon scattering is elastic, the maximum energy in any photon-photon collision is $2\Gamma\epsilon_{\rm sn}$, which for $\Gamma \sim 20$ and $\epsilon_{\rm sn} \sim 1\,{\rm keV}$ is insufficient to pair produce.

---

[2] Note that this is in contrast to many of the theoretical estimates in the literature in which behaviour expected by one-dimensional models is $\Gamma \to \sigma^{1/3}$ (see, e.g., Michel 1969; Goldreich & Julian 1970; Begelman & Lee 1994; Beskin et al. 1998). Spitkovsky & Arons (2004) claim that the discrepancy is largely due to the various artificial assumptions that these early efforts necessarily adopted, including spherical symmetry, split-monopole field configurations, and the region of applicability of the force-free approximation.

Nonetheless, for a thermal seed photon distribution a high energy tail will exist, including photons with $\epsilon > m_e c^2/\Gamma$ and hence will be able to pair produce. The number density of such photons accumulated in the jet frame by the end of the burst is roughly given by

$$n_\epsilon \simeq g\Gamma \frac{u_T}{kT_\gamma} \frac{v_{\rm sn}}{c} \left(\frac{m_e c^2}{\Gamma k T_\gamma}\right)^2 \exp\left(-\frac{m_e c^2}{\Gamma k T_\gamma}\right) , \qquad (35)$$

where the factor of $v_{\rm sn}/c$ accounts for the fact that in the jet the photons are free streaming and $g \simeq 0.15$ is a normalisation factor. The resulting optical depth to pair production is then $\sigma_T n_\epsilon r/\Gamma$, where r is the radius in the lab frame (see, e.g., Lithwick & Sari 2001). Therefore, the lepton density at the end of the burst as a result of photon annihilation is $n_{e^\pm} \simeq \sigma_T n_\epsilon^2 r/\Gamma$, with an associated optical depth along the jet of

$$\begin{aligned} \tau &\simeq \frac{1}{2\Gamma}\sigma_T n_{e^\pm} r \\ &\simeq \frac{1}{2}\left(\sigma_T n_\epsilon \frac{r}{\Gamma}\right)^2 \\ &\simeq 3\times 10^{-3} , \end{aligned} \qquad (36)$$

for $r \simeq 10^{12}\,{\rm cm}$. Note that since pair annihilation has been ignored, this is only an upper limit. Thus, it may be safely concluded that pair production is insignificant during the the burst.

In general, both the jet and the seed photon density and temperature will be expected to have radial structure. In the jet this is due to competition between the magnetic stresses and the Compton drag. In the seed photons this is due to the adiabatic cooling of the supernova ejecta. A direct result of this structure is that, despite beginning with thermal seed photons, the time integrated spectra can have the observed broken power law shape where the break energy could indeed be interpreted as the temperature of the up-scattered seed photons when $\tau_\parallel \simeq 1$, i.e., roughly $2\Gamma^2\,{\rm keV} \sim {\rm few}\times 10^2\,{\rm keV}$. For the case where the seed photon temperature has a radial power-law dependence this has already been explicitly shown to be the case by Ghisellini et al. (2000). However, in this scenario, since the density of seed photons depends upon distance from the helium star, different orientations of the jet with respect to the orbital plane will lead to substantial changes in the spectral slopes of the integrated emission. Thus, because the compact object is expected to have suffered a kick during its birth, the considerable variation observed in burst spectral slopes would be expected.

3.5 Population Statistics

For a given beaming angle ($\sim \Gamma^{-1}$) approximately $10^{-10}\Gamma^2$ bursts occur per galaxy per year (Schmidt 2001). This implies that the formation rate ($\mathcal{R}_{\rm CO-He}$) for the progenitor systems satisfy

$$\mathcal{R}_{\rm CO-He} \gtrsim 4\times 10^{-8} \left(\frac{\Gamma}{20}\right)^2 {\rm galaxy}^{-1}{\rm yr}^{-1} . \qquad (37)$$

There is a considerable literature which addresses the formation rates of neutron star–neutron star binaries and neutron star–black hole binaries. Because in both cases it is believed that these are produced by the evolution of compact object–Helium star binaries, the formation rates of the former place lower limits upon the formation rate of the latter. Therefore, the progenitor formation rate must be compared to $\mathcal{R}_{\rm NS-NS} \simeq 10^{-6}$ to $5\times 10^{-4}\,{\rm galaxy}^{-1}{\rm yr}^{-1}$ (Kalogera et al. 2004) and $\mathcal{R}_{\rm NS-BH} \gtrsim 10^{-4}\,{\rm galaxy}^{-1}{\rm yr}^{-1}$ (Bethe & Brown 1998). Hence, there are more than enough presumed compact object–Helium star products to account for the number of γ-ray bursts observed. It should also be noted that the formation rate of compact binaries is expected to be considerably smaller than the formation rate of the progenitor binaries due to the possibility of unbinding the progenitor as a consequence of the ensuing supernova, and the fact that the black hole–black hole binaries have been ignored.

4 AFTERGLOW

A consequence of electromagnetic domination in the jet is the absence of internal shocks as long as the jet remains relativistic. However, as the jet cools, the flow will become increasingly hydrodynamic. When Γ is of order unity, strong internal shocks may be expected to develop. At this point the internal kinetic energy of the jet can be thermalised, producing a moderately relativistic fireball, which can then be analysed within the highly successful standard fireball afterglow model (see, e.g., Mészáros 2002; Königl & Granot 2002 argue that many of the diverse afterglow phenomena can be naturally produced if the afterglow is produced inside of a pulsar-wind bubble). Due to the velocity gradient at the end of the jet, when enough matter accumulates a Compton thick head will develop, shutting off further prompt emission. This can be expected to occur over the time scale for the jet to proceed from the radius at which $\tau_\parallel \simeq 1$ ($\sim 10^{11}\,{\rm cm}$) to the radius at which $\Gamma \sim 1$ ($\sim 10^{12}\,{\rm cm}$), which for the scenario considered here is approximately $30-100\,{\rm s}$. After this time, the jet will continue to pump energy into the growing fireball at its head. Only when the rotational energy of the compact object is sufficiently exhausted, or accretion ceases, will the jet cease and the fireball expand under its own pressure. For a neutron star this also can be expected to occur over a comparable time scale as the prompt emission, while for a black hole this can continue considerably longer (see section 2).

5 MODEL IMPLICATIONS

This model has a number of direct observational implications discussed below, many of which have already been detected.

5.1 Burst Substructure

The fact that the ejecta is Thomson thick and inhomogeneous leads to considerable burst substructure. In this case seed photons will not be continuously available, but rather will enter the jet in bunches over timescales (δt) associated with the inhomogeneity length scales (ℓ), i.e.,

$$\delta t \simeq \frac{\ell}{v_{\rm sn}} \sim 1\,{\rm s}\,, \tag{38}$$

implying

$$\ell \sim 10^3\,{\rm km} \sim 10^{-3} R_{\rm He}\,. \tag{39}$$

This will occur when an ejecta clump impacts the jet and is subsequently either sheared apart, releasing the entrained photons, or forms strong shocks and thus thermalising its bulk kinetic energy.

To lowest order, the rate of supplied seed photons may be treated as uniform over δt and vanishing otherwise. In this case, for a single clump, the number of seed photons within the jet will evolve according to

$$\frac{{\rm d}N_{\rm seed}}{{\rm d}t} = \begin{cases} \dfrac{\mathcal{N}}{\delta t} - \dfrac{\tau_b}{\delta t} N_{\rm seed} & 0<t<\delta t \\ -\dfrac{\tau_b}{\delta t} N_{\rm seed} & \delta t < t \end{cases}, \tag{40}$$

where $\mathcal{N}$ is the total number of seed photons in the clump and

$$\tau_b = \tau_\perp \frac{\Gamma c \delta t}{2r}\,, \tag{41}$$

which is expected to be ~ 0.3 at the point where most of the emission occurs. The solution is trivially found to be

$$N_{\rm seed} = \mathcal{N} {\rm e}^{\tau_b t/\delta t} \begin{cases} \dfrac{t}{\delta t} & 0<t<\delta t \\ 1 & \delta t < t \end{cases}. \tag{42}$$

Since nearly every seed photon that enters the jet will be upscattered to γ-ray energies, this also provides the expected light curve for a single subpulses

$$\frac{{\rm d}N_\gamma}{{\rm d}t} = f \frac{\tau_b}{\delta t} N_{\rm seed}\,. \tag{43}$$

where f is the fraction of singly scattered photons and is typically of order unity. This has the fast rise–exponential decay structure observed (cf. Norris et al. 1996). Furthermore, the ratio of the exponential decay time to the (approximately) linear rise time is $\tau_b^{-1} \sim 3$, as observed (Norris et al. 1996). As the jet Lorentz factor increases these subpulses would be expected to be systematically more symmetric for a given inhomogeneity scale in the supernova ejecta (which would not be expected to vary considerably). Thus, more energetic bursts would be expected to produce more symmetric subpulses, which has also been observed (Norris et al. 1996).

5.2 Time Lags and Energy Dependent Subpulse Widths

Photons at energies below $2\Gamma^2 T_\gamma$ will be due to both the low energy tail of the seed photon distribution and multiple scatters both within the jet and at the jet boundaries. The high bulk Lorentz factor of the jet implies that the scattering angles will typically be on the order of Γ^{-1}. Therefore, for each encounter

$$\epsilon_f \simeq \frac{\epsilon_i}{1+\Gamma\epsilon_i/m_e c^2}\,. \tag{44}$$

Many encounters may be approximated by integrating the equation

$$\frac{{\rm d}\epsilon}{{\rm d}N_{\rm scat}} \simeq \frac{\epsilon}{1+\Gamma\epsilon/m_e c^2} - \epsilon\,, \tag{45}$$

to give

$$N_{\rm scat} \simeq \frac{m_e c^2}{\Gamma}\left(\frac{1}{\epsilon} - \frac{1}{\epsilon_{\rm peak}}\right) - \ln\left(\frac{\epsilon}{\epsilon_{\rm peak}}\right) \sim \frac{m_e c^2}{\Gamma\epsilon}\,, \tag{46}$$

and thus $\epsilon \sim N_{\rm scat}^{-1}$ in the limit of many scatters. Due to the additional path length traversed by these photons, they will lag behind the single scattered photons by a time $\propto N_{\rm scat}$. In addition, since the scattered photons are performing a biased random walk, they will spread in time $\propto N_{\rm scat}^{1/2}$. This gives the following scalings

$$\Delta t_{\rm lag} \propto \Gamma^{-1}\epsilon^{-1}\,, \tag{47}$$

and

$$\delta t \propto \Gamma^{-1/2}\epsilon^{-1/2}\,, \tag{48}$$

where the former is consistent with the observed anti-correlation between the time lags and the overall luminosity of the burst (Band 1997), and the latter is in rough agreement with the observed relation $\partial \ln \delta t/\partial \ln \epsilon \simeq -0.4$ (Fenimore et al. 1995). The relevant time scales for the time lag can be estimated directly by noting that the jet width is roughly

$$\frac{r}{\Gamma} \sim 5\times10^9 \left(\frac{\Gamma}{20}\right)^{-1} \left(\frac{r}{10^{11}\,{\rm cm}}\right)\,{\rm cm}\,, \tag{49}$$

and hence the lower energy emission will lag by $N_{\rm scat}(r/\Gamma c) \sim 0.2 N_{\rm scat}$ s. If a majority of the low energy photons are produced deeper within the jet (where the Compton depth is higher), this time scale can decrease by an order of magnitude. In either case this is again consistent with observations of burst pulse time lags (Band 1997).

5.3 Spectral Softening

As the jet evolves, its axial optical depth will increase and the position at which the majority of the emission arises from will move outward towards regions of lower Lorentz factor. Near the end of the burst the Lorentz factor at the γ-ray photosphere is expected to be no more than a few. As a result, the emission can be expected to soften considerably as the burst proceeds. The rate at which this softening occurs depends upon the radial structure of the jet as discussed in section 3.4 and would be expected to vary considerably between bursts.

5.4 Peak–Inferred Isotropic Energy Relation

Amati et al. (2002) (and more recently Amati 2004) have reported a correlation between the peak spectral energy and the inferred isotropic energy of bursts, namely $\epsilon_{\rm peak} \propto E_{\rm iso}^{1/2}$. In the context of the model presented here, this would be naturally expected if the dominant factor in the variation between bursts was the maximum jet Lorentz factor. This is not unexpected if the helium star supernovae are similar, implying that scatter in the orbital separation and compact object parameters, both of which enter most significantly into the determination of Γ, produces the variability amongst bursts. Then, in terms of the typical seed photon energy ($\epsilon_{\rm sn}$), the peak γ-ray energy is

$$\epsilon_{\rm peak} \simeq 2\Gamma^2 \epsilon_{\rm sn} \,. \tag{50}$$

From equation (34) it is clear that

$$L_{\rm iso} \simeq 8\Gamma^4 \left(u_T + u_S\right) v_{\rm sn} r^2 \propto \epsilon_{\rm peak}^2 \,, \tag{51}$$

where the last proportionality holds if the typical ejecta densities and velocities and the radius at which the jet becomes optically thick are similar amongst bursts. This may be trivially inverted to yield the observed relation.

5.5 X-ray Flash Characteristics

For jet Lorentz factors $\sim$ few, the peak of the emission would occur in the X-rays, and thus this model provides a natural explanation for X-ray flashes. Note that this is neither a structured nor uniform jet model (cf. Rossi et al. 2002; Lamb et al. 2004). In the former, viewing an azimuthally structured jet from different angles provides the peak–inferred isotropic energy relation. In the latter, the distribution is in the opening angle of the jet. In both it is assumed that there is little scatter in the total energy of the burst. In contrast, as seen in equation (34) with the same assumptions made in the previous subsection, in the scenario presented here the energy released in the form of γ-rays is expected to scale as

$$L_{\rm jet} \propto \Gamma^{-2} \,. \tag{52}$$

However, in this as well as in the normal bursts, this energy is expected to be subdominant relative to the energy in the supernova itself.

Since X-ray flashes share many of the temporal and spectral features of γ-ray bursts, including lying upon the peak–inferred isotropic luminosity relation of Amati (2004), it is tempting to interpret them as simply subluminous bursts. Recently, the bolometric energy of the X-ray flash XRF 020903 has been measured and was indeed found to be similar to typical γ-ray bursts despite having a substantially lower inferred isotropic luminosity (Soderberg et al. 2004).

5.6 Late Light Curve Variability

Despite the large amount of energy released in the supernova, the binary does not necessarily become unbound (indeed, it must not if this is a viable formation scenario for double pulsars). Therefore, in systems with a sizable amount of ejecta remaining in the vicinity of a nascent compact remnant, variability due to the occasional accretion by the companion compact object may be expected after the supernova becomes optically thin, and thus late in the light curve. This may explain the late time (~ 50 days after the burst) variability observed in the residual light curve of SN 2003dh, which has a rough time scale of a few days, implying an orbital separation of $\sim 10^{12}$ cm, in agreement with what would be expected in this model (Matheson et al. 2003).

5.7 Polarisation

Lazzati et al. (2004) have shown that inverse-Compton scattering by jets can produce large degrees of linear polarisation ($\sim 100\%$ in some cases). This is a direct result of the relativistic aberration of the seed photons in the jet frame and is a function of the viewing angle of the jet, nearing unity for $\theta \sim \Gamma^{-1}$. Therefore, jet models in which the prompt emission is due to inverse-Compton scattering will generally exhibit wide variation in the degree of linear polarisation, ranging from zero along the jet axis to unity along the jet edge. As a consequence, the degree of linear polarisation may be used to measure the jet viewing angle, breaking the degeneracy between azimuthal jet structure and low luminosity in attempts to utilise γ-ray bursts as cosmological standard candles. Since, in the model presented here, the spectral evolution of each subpulse to lower energy is due to multiple scatterings, the polarisation fraction would be expected to decrease roughly exponentially with the number of scatters and thus the polarisation should be a strong function of energy as well.

Note that as long as the seed photon frequency in the jet frame is much greater than the cyclotron frequency, as is expected to be the case when the jet is optically thin axially (see equation 22), the magnetic field will not significantly effect the polarisation properties of the prompt emission.

Presently, the only measurement of the prompt emission polarisation involved GRB 021206 and was found to be $80\% \pm 20\%$ by Coburn & Boggs (2003) (though this claim continues to be controversial). However, due to the large uncertainty this may be consistent with both synchrotron self-Compton models and the model presented here. If this is confirmed in future bursts, this would provide strong evidence for Comptonised jet models.

6 CONCLUSIONS

Rough estimates of the consequences of supernovae in compact object–helium star binaries have been used to suggest that such an event is a viable candidate for γ-ray bursts. Such events are assumed to occur in the standard double pulsar evolution scenario. Within this context a number of population calculations have been performed, implying that indeed these events are likely to be frequent enough to explain the number of bursts seen. This model is capable of explaining a number of the burst characteristics, including the subpulse light curves and energy dependence, late time spectral softening, and the peak–inferred isotropic energy relation. In addition, X-ray flashes and γ-ray bursts are naturally combined into a single unified theory, as recently suggested by observations.

If the binary remains bound, as is necessarily the case for the double pulsar formation scenarios, late time variability may be expected. Such variability has been observed in the light curve of GRB 030329/SN 2003dh. While no clear periodicity is discernible, the typically time scales are consistent with an orbital separation $\sim 10^{12}$ cm as expected by this model. Future observations of late time afterglow light curves can provide evidence for the existence of binaries in γ-ray burst progenitors.

The prediction of significant degrees of polarisation in Compton dragged jet models in general, and this model in particular, is noteworthy. In the absence of strong structure within the jet, this would necessarily lead to significant variation in the degree of polarisation, ranging from zero to unity. Predictions for significant degrees of polarisation which depend upon viewing angle has significant implications for cosmological observations. Even in the absence of a detailed understanding of the azimuthal jet structure, polarisation provides a simple way in which to identify the viewing angle, removing this degeneracy. Unfortunately, due to its considerable uncertainty, the only measurement of prompt emission polarisation is as yet unable to differentiate between synchrotron self-Compton models and Comptonised jet models. Thus, clearly future polarisation observations are required as well.

Many of the observational predictions of this model are generic to Compton dragged jets. These include the spectrum (Ghisellini et al. 2000), polarisation (Lazzati et al. 2004), subpulse lags, and subpulse energy dependence (cf. Dado et al. 2002). To a lesser extent, the Amati relation, and thus the X-ray flash characteristics, is also generally expected as long as the primary difference among bursts is the jet Lorentz factor.

This model is also very similar to the collapsar, with the obvious difference that in this case the compact object is outside the helium star (which need not be a Wolf-Rayet star here). As such, the most immediate feature of the collapsar model, the association with supernova, is present here as well. However, it is not possible to simply subsume this model into the collapsar by placing the compact object within the helium star; the primary difficulty being that the solution to the compactness problem would no longer apply due to the considerable supply of MeV photons in the central regions of the supernova. As a result the jet would remain optically thick until radii two orders of magnitude larger than those considered here. Considering the likely fact that the supernova ejecta are travelling radially from the compact object at this point, the mechanism proposed here for producing the burst substructure will be unlikely to work.

Unique to this model is the manner in which the successes of Comptonised jet and collapsar models are unified. Furthermore, it provides a natural class of progenitors, in which supernovae are already believed to occur as a result of independent observational evidence. Thus, the results presented here may be regarded as both a proposal for an new γ-ray burst mechanism and an investigation into the observational consequences of what appears to be an inevitable process given the currently observed double neutron star systems.

ACKNOWLEDGEMENTS

I would like to thank a number of people with whom I've had useful discussions, including Jon McKinney, Ramesh Narayan, Andrew McFadyen, Roger Blandford, Max Lyutikov, Yasser Rathore, Gerry Brown, and Ralph Wijers. I would also like to thank the anonymous referee who's suggestions substantially improved this manuscript. I would especially like to thank Martin Rees for a number of insightful conversations and generously hosting me during the time that much of this work was completed. This research was supported by NASA-ATP grant NAG5-12032 and NSF RTN grant AST-9900866.

REFERENCES

Amati L., 2004, Chin. J. Astron. Astrophys., 3, 455
Amati L., Frontera F., Tavani M., in't Zand J. J. M., Antonelli A., Costa E., Feroci M., Guidorzi C., Heise J., Masetti N., Montanari E., Nicastro L., Palazzi E., Pian E., Piro L., Soffitta P., 2002, A&A, 390, 81
Band D. L., 1997, ApJ, 486, 928
Begelman M. C., Lee Z.-Y., 1994, ApJ, 426, 269
Begelman M. C., Sikora M., 1987, ApJ, 322, 650
Berger E., Kulkarni S. R., Frail D. A., 2004, ApJ, 612, 966
Beskin V. S., Kuznetsova I. V., Rafikov R. R., 1998, MNRAS, 299, 341
Bethe H. A., Brown G. E., 1998, ApJ, 506, 780
Blandford R. D., Znajek R. L., 1977, MNRAS, 179, 433
Chevalier R. A., 1989, ApJ, 346, 847
Coburn W., Boggs S. E., 2003, Nature, 423, 415
Dado S., Dar A., De Rújula A., 2002, A&A, 388, 1079
Eichler D., Livio M., Piran T., Schramm D. N., 1989, Nature, 340, 126
Ekşi K. Y., Hernquist L., Narayan R., 2005, ApJ, 623, L41
Fenimore E. E., in 't Zand J. J. M., Norris J. P., Bonnell J. T., Nemiroff R. J., 1995, ApJL, 448, L101+
Frail D. A., Kulkarni S. R., Sari R., Djorgovski S. G., Bloom J. S., Galama T. J., Reichart D. E., Berger E., Harrison F. A., Price P. A., Yost S. A., Diercks A., Goodrich R. W., Chaffee F., 2001, ApJL, 562, L55
Fryer C. L., Benz W., Herant M., 1996, ApJ, 460, 801
Gammie C. F., Shapiro S. L., McKinney J. C., 2004, ApJ, 602, 312
Ghisellini G., Lazzati D., Celotti A., Rees M. J., 2000, MNRAS, 316, L45
Ghosh P., Lamb F. K., 1979, ApJ, 232, 259
Goldreich P., Julian W., 1970, ApJ, 160, 971
Hawley J. F., Balbus S. A., 1995, Publications of the Astronomical Society of Australia, 12, 159
Heinz S., Begelman M. C., 1999, ApJL, 527, L35
Königl A., Granot J., 2002, ApJ, 574, 134
Kalogera V., Kim C., Lorimer D. R., Burgay M., D'Amico N., Possenti A., Manchester R. N., Lyne A. G., Joshi B. C., McLaughlin M. A., Kramer M., Sarkissian J. M., Camilo F., 2004, ApJL, 601, L179
Klebesadel R. W., Strong I. B., Olson R. A., 1973, ApJL, 182, L85+
Komissarov S. S., 2004, MNRAS, 350, 1431
Komissarov S. S., Lyubarsky Y. E., 2004, MNRAS, 349, 779
Kouveliotou C., Meegan C. A., Fishman G. J., Bhat N. P., Briggs M. S., Koshut T. M., Paciesas W. S., Pendleton G. N., 1993, ApJL, 413, L101
Lamb D. Q., Donaghy T. Q., Graziani C., 2004, New Astronomy Review, 48, 459
Lazzati D., Ghisellini G., Celotti A., 1999, MNRAS, 309, L13
Lazzati D., Rossi E., Ghisellini G., Rees M. J., 2004, MNRAS, 347, L1
Levinson A., 2005, astro-ph/0502346
Li Z.-Y., Chevalier R. A., 2003, Lecture Notes in Physics, Berlin Springer Verlag, 598, 419
Lithwick Y., Sari R., 2001, ApJ, 555, 540
Mészáros P., 2002, ARAA, 40, 137
MacFadyen A. T., Woosley S. E., Heger A., 2001, ApJ, 550,

410

Matheson T., Garnavich P. M., Stanek K. Z., Bersier D., Holland S. T., Krisciunas K., Caldwell N., Berlind P., Bloom J. S., Bolte M., Bonanos A. Z., Brown M. J. I., Brown W. R., et al., 2003, ApJ, 599, 394

McKinney J. C., 2005, *private communication*

McKinney J. C., Gammie C. F., 2004, ApJ, 611, 977

Michel F. C., 1969, ApJ, 158, 727

Misner C. W., Thorne K. S., Wheeler J. A., 1973, Gravitation. W.H. Freeman and Co., San Francisco

Narayan R., Paczynski B., Piran T., 1992, ApJL, 395, L83

Norris J. P., Nemiroff R. J., Bonnell J. T., Scargle J. D., Kouveliotou C., Paciesas W. S., Meegan C. A., Fishman G. J., 1996, ApJ, 459, 393

Paczynski B., 1991, Acta Astronomica, 41, 257

Piran T., 2004, Rev. Modern Phys., 76, 1143

Popham R., Woosley S. E., Fryer C., 1998, ApJ, 518, 356

Romanova M. M., Ustyugova G. V., Koldoba A. V., Lovelace R. V. E., 2004, ApJL, 616, L151

Rossi E., Lazzati D., Rees M. J., 2002, MNRAS, 332, 945

Sakamoto T., Lamb D. Q., Graziani C., Donaghy T. Q., Suzuki M., Ricker G., Atteia J., Kawai N., Yoshida A., Shirasaki Y., Tamagawa T., Torii K., Matsuoka M., Fenimore E. E., Galassi M., Doty J., et al., 2004, astro-ph/0409128

Schmidt M., 2001, ApJL, 559, L79

Soderberg A. M., Kulkarni S. R., Berger E., Fox D. B., Price P. A., Yost S. A., Hunt M. P., Frail D. A., Walker R. C., Hamuy M., Shectman S. A., Halpern J. P., Mirabal N., 2004, ApJ, 606, 994

Spitkovsky A., Arons J., 2004, ApJ, 603, 669

Thompson C., 1994, MNRAS, 270, 480

Thompson T. A., Chang P., Quataert E., 2004, ApJ, 611, 380

Usov V. V., 1992, Nature, 357, 472

Vietri M., Stella L., 1998, ApJL, 507, L45

Vlahakis N., 2004, ApJ, 600, 324

This paper has been typeset from a TEX/ LATEX file prepared by the author.